

To see the latest GeoStudio learning content, visit <u>Seequent Learning Centre</u> and search the catalogue for "GeoStudio".

Introduction

The International Conference on Geotechnical and Geological Engineering was held in Melbourne, Australia in November 2000. The conference is referred to here as GeoEng2000. A series of invited keynote lectures were presented at the conference. One of the keynote lectures was titled Computing and Computer Modelling in Geotechnical Engineering (Carter et al. 2000). One of the topics of this keynote paper was *Validation and Calibration of Computer Simulations*, which included a summary of the work by the German Society for Geotechnics on establishing some benchmark problems for validating numerical analyses.

One of the benchmark examples involved simulating the construction of a tie-back wall for a deep excavation in Berlin. Numerous people from universities and consulting companies simulated the construction history based on curated geotechnical data. The simulated lateral wall deflections, along with surface settlements and structural forces, were submitted to the organizing body for comparison with the measured data. The objective of this example is to demonstrate how GeoStudio can be used to simulate this problem. More specifically this example will be used to:

- Demonstrate the various features of GeoStudio that can be used to simulate an excavation construction history involving dewatering;
- Highlight some of the most important aspects of modelling an excavation construction history involving a tie-back wall with pre-stressed anchors.

Background

Figure 1 shows a schematic diagram of the tie-back wall. The geology consists of Berlin sand, with the water table originally 3 m below the ground surface. The excavation was completed in four stages to a depth of 16.8 m. The diaphragm wall was supported by three rows of anchors that were pre-stressed and spaced in the out-of-plane direction as shown in Figure 1.

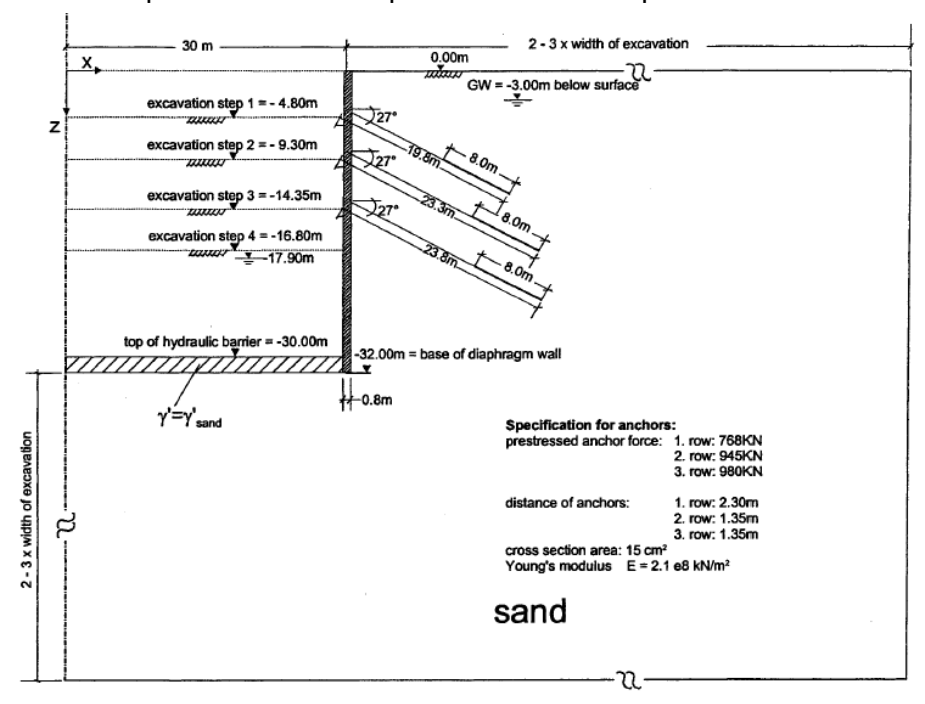


Figure 1. Schematic of the Berlin tie-back wall.



Carter et al. (2000) provided these properties for the diaphragm wall:

- E = $30,000 \text{ MPa} = 30,000,000 \text{ kPa} = 3 \times 10^7 \text{ kPa}$ (typical of concrete)
- Poisson's ratio (v) = 0.15
- Unit weight $(y) = 24 \text{ kN/m}^3$
- Angle of wall friction = $\phi/2$
- In-plane thickness = 0.8 m

The free end of the anchors have a cross-sectional area of 15 cm 2 (1.5 x 10 3 m 2) and an elastic modulus E = 2.1 x 10 8 kPa (Figure 1). The out-of-plane spacing and pre-stress forces of each row of anchors is shown in Figure 1.

The Berlin sand is of medium density with the following measured/approximated properties:

- $\phi' = 35^{\circ}$
- $K_0 = 1 \sin \phi' = 0.43$
- $\gamma' = 19 \text{ kN/m}^3$

The soil stiffness is a critical parameter in this analysis. The suggested variation in the elastic modulus for the sand was (Carter et al., 2000; Figure 2):

- $E = 20,000 \text{ x z}^{0.5}$ for 0 < z <= 20 m (where z = depth below ground); and,
- E = $60,000 \times z^{0.5}$ for z > 20 m.

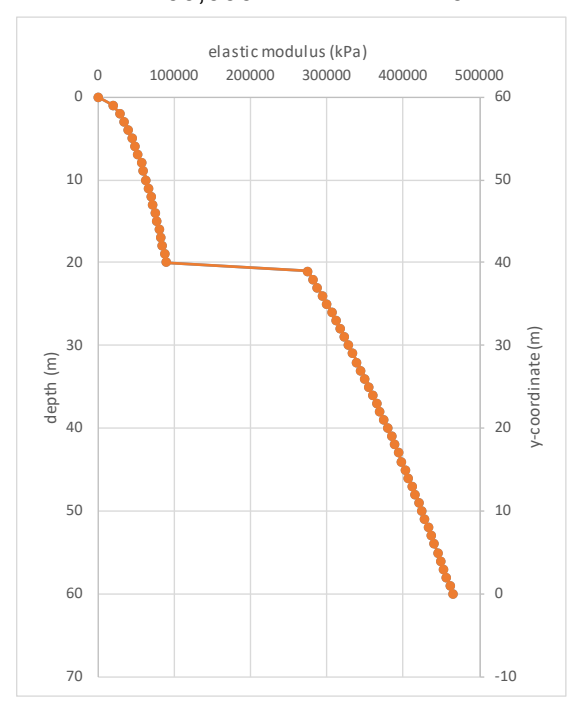


Figure 2. Specified variation of soil stiffness (E) with depth.

Figure 3 shows the general assumptions and recommended computation steps from Carter et al. (2000). The hydraulic barrier was installed to prevent water from flowing up into the excavation. The water level in the excavation was lowered in stages during construction; however, Carter et al. (2000) suggested that dewatering be simulated in one stage. Note also that a) the initial horizontal effective stresses were to be commensurate with the earth pressure coefficient; and, b) the hydraulic cut-off was assumed to provide no structural support.



9.4.1 General Assumptions

Additional specifications for this example are as follows:

- · plane strain conditions could be assumed,
- any influence of the diaphragm wall construction could be neglected, i.e., the initial stresses were
 established without the wall, and then the wall was "wished-in-place" and its different unit weight
 incorporated appropriately,
- the diaphragm wall could be modelled using either beam or continuum elements,
- interface elements existed between the wall and the soil,
- the domain to be analysed was as suggested in Figure 59,
- the horizontal hydraulic cut-off that existed at a depth of -30.00 m was not to be considered as structural support, and
- · the pre-stressing anchor forces were given as design loads.

9.4.2 Computational Steps

The following computational steps had to be performed by the various analysts:

- the initial stress state was given by σ_ν = γH, σ_h = K_oγH,
- the wall was "wished-in-place" and the deformations reset to zero,
- construction stage 1: groundwater-lowering to -17.90 m,
- construction stage 2: excavation step 1 (to level -4.80 m),
- construction stage 3: activation of anchor 1 at level –4.30 m and prestressing,
- construction stage 4: excavation step 2 (to level -9.30 m),
- construction stage 5: activation of anchor 2 at level –8.80 m and prestressing,
- construction stage 6: excavation step 3 (to level -14.35 m),
- construction stage 7: activation of anchor 3 at level –13.85 m and prestressing, and
- construction stage 8: excavation step 4 (to level –16.80 m).

The length of the anchors and their prestressing loads are indicated in Figure 59.

Figure 3. Excerpt from Carter et al. (2000) showing some general assumptions and the recommended computation steps.

Numerical Simulation

Figure 4 shows the geometry required to simulate the excavation stages and anchor activations. The details of the project's definition can be explored by opening the associated file. The geometry was defined by rounding to the nearest metre. The entire construction sequence is duplicated in the project file so that the Berlin sand could be represented by the Mohr-Coulomb and Hardening Soil models. The Mohr-Coulomb model was parameterized using the aforementioned properties, which are summarizing in Table 1. The domain was split at an elevation of 40 m (i.e. depth of 20 m) to accommodate parameterization of the Hardening Soil model (Figure 5). Table 2 shows the parameterization of the Hardening Soil model for depths less than and greater than 20 m, which is where the demarcation in stiffness occurs (Figure 2). The exponent m was set to 0 for the upper unit to improve convergence during the water pressure decrement.



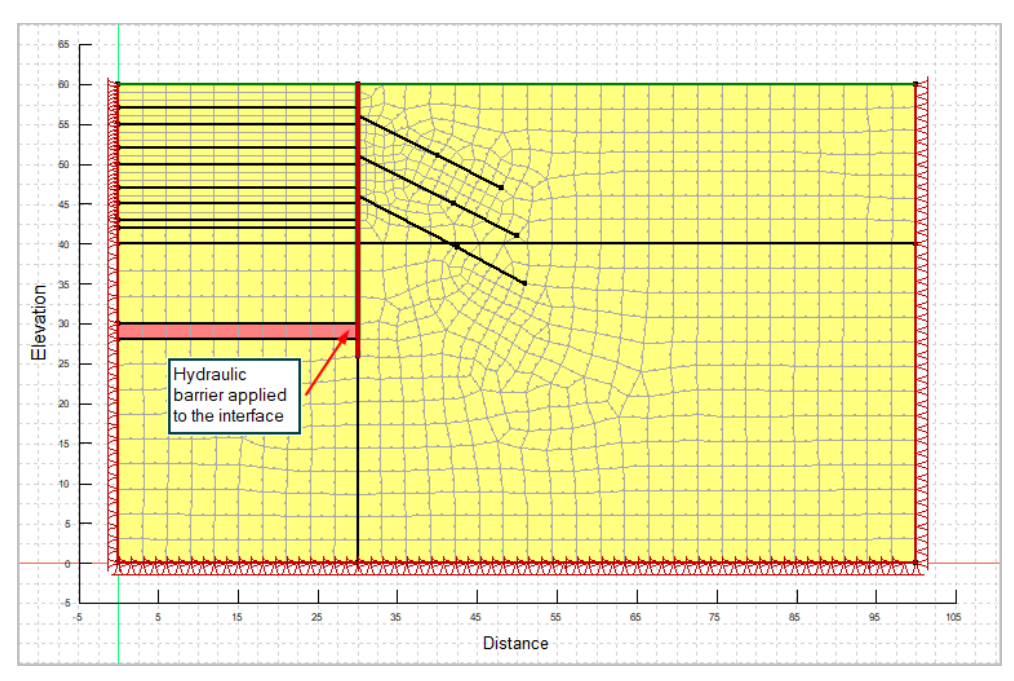


Figure 4. Geometry and excavation stages for the tied back excavation simulated using the Mohr-Coulomb model.

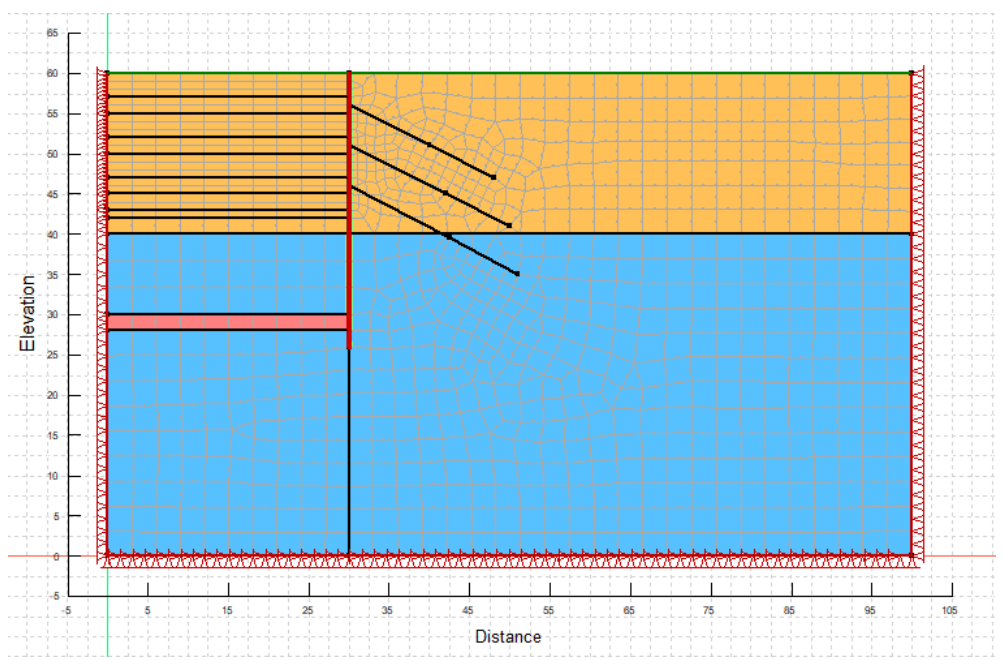


Figure 5. Geometry and excavation stages for the tied back excavation simulated using the Hardening Soil model.



Table 1. Mohr-Coulomb parameters used to represent the Berlin Sand.

Parameter	Mohr-Coulomb model
Unit weight (kN/m3)	20
Initial void ratio	0.5
Effective Elastic modulus E' (kPa)	Figure 2
Effective Cohesion c' (kPa)	1
Effective Friction angle ϕ'	35
Dilation angle ψ	10
Poisson's ratio v'	0.2
K_{0}^{nc}	0.4264

Table 2. Hardening Soil parameters used to represent the Berlin Sand.

Parameter	Depth < 20 m	Depth > 20 m	
Unit weight (kN/m3)	20	20	
Initial void ratio	0.5	0.5	
O.C. Ratio	1.0	1.0	
E_{50}^{ref} (kPa)	32000	96000	
E ^{ref} _{oed} (kPa)	32000	96000	
E_{ur}^{ref} (kPa)	192000	384000	
Reference pressure (kPa)	100	100	
Power m	0.0	0.5	
Effective Cohesion c' (kPa)	1	1	
Effective Friction angle ϕ'	35	35	
Dilation angle ψ	10	10	
Poisson's ratio v'	0.2	0.2	
Failure ratio R_f	0.9	0.9	
K_{0}^{nc}	0.4264	0.4264	

The hydraulic barrier at the base of the diaphragm wall was represented by the Mohr-Coulomb



material model (Table 1). The soil-structure interface was also represented by a Mohr-Coulomb model with a constant, and reduced, stiffness and an effective friction angle of ½ of that of the Berlin sand (Carter et al. 2000; Figure 4). The hydraulic properties of the Berlin sand (and wall interface) were represented by the Saturated/Unsaturated model with an estimated volumetric water content function and constant hydraulic conductivity of 1 m/d. The hydraulic properties of the hydraulic barrier were represented by the Saturated-Only model with an arbitrarily low hydraulic conductivity of 1.0E-6 m/d. Notice that the hydraulic barrier was applied to the interface elements on the left side of the diaphragm wall (Figure 4).

The diaphragm wall and grouted portions of the anchors are represented by structural beam elements (Table 3). The free portions of the anchors are represented by structural bar elements (Table 3). The diaphragm wall has a thickness of 0.8 m, resulting in an out-of-plane cross-sectional area of 0.8 m², and a geometric moment of inertia of

 $I_{zz} = b^3 h/12 = 0.8^3 (1.0)/12 = 4.3E - 02$ m^4 (Note: bending is about the out-of-plane zz axis). The stiffness E of the grouted and free portions of the anchors were assumed equivalent. The area of the grouted portion was assumed to be 3 times that of the bar (i.e. 3×15 cm^2 = 45 cm^2). The geometric moment of inertia of the grouted portions are therefore calculated as $I_{zz} = \pi d^2/4 = 4E - 05$ m/4. The pre-stress force for each raw of anchors is permelized by

 $I_{zz}=\pi d^2/4=4E-05$ m^4. The pre-stress force for each row of anchors is normalized by spacing at solve time; consequently, the input value matches the measured value. The difference between the unit weight of the wall and soil is ignored in the analysis and Poisson's ratio is implicitly zero in the beam element formulation.

Table 3. Parameters of the structura	l elements used to represent th	ne diaphragm wall and anchors.
--------------------------------------	---------------------------------	--------------------------------

Structure	E (kPa)	A (m²)	I (m ⁴)	Spacing (m)	Prestress (kN)
Diaphragm Wall	3.0 x 10 ⁷	0.8	4.3 x 10 ⁻²	1	N/A
Anchors – Row 1	2.10 x 10 ⁸	0.0015 / 0.0045	4.0 x 10 ⁻⁵	2.3	768
Anchors – Row 2	2.10 x 10 ⁸	0.0015 / 0.0045	4.0 x 10 ⁻⁵	1.35	945
Anchors – Row 3	2.10 x 10 ⁸	0.0015 / 0.0045	4.0 x 10 ⁻⁵	1.35	945

Figure 6 shows the analysis tree. The initial stresses were established using the K0 Procedure of the In Situ analysis type (GEOSLOPE International Ltd., 2020a). The *in situ* water pressures were defined using a water table at an elevation of 57 m. A load-deformation analysis was subsequently used to simulate the stress-strain response resulting from dewatering the excavation. The fluid pressure increment is calculated by the solver from the difference between the final and initial (i.e. *in situ*) water pressures. The final dewatered pore-water pressure regime was simulated using a steady-state SEEP/W analysis, which required a far-field total head on the right boundary (h = 57 m) and a zero water pressure boundary condition under the base of the final excavation (el. 17.9 m; Figure 1). The diaphragm wall was designated an impervious barrier (GEOSLOPE International Ltd., 2020b) to force flow under the wall and through the hydraulic barrier. The subsequent analyses in the tree involve either excavation or installation and pre-stressing of the anchors. Note that the diaphragm wall and hydraulic barrier were wished-into-place during the simulation of dewatering.



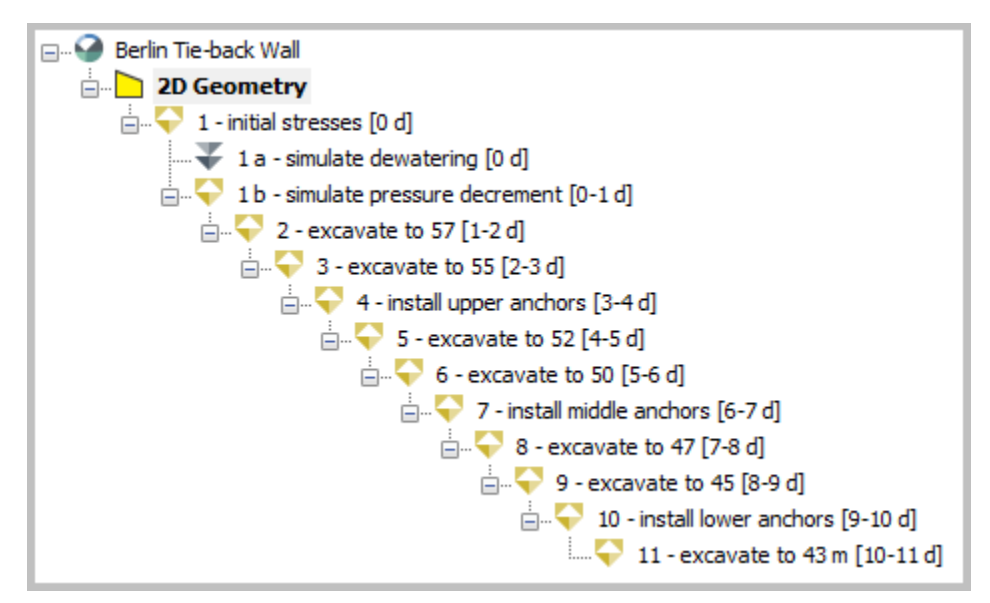


Figure 6. Analysis Tree for the Project.

Results and Discussion

Figure 7 compares a subset of simulations by consultants and academics to the measured inclinometer data. Simulations showing excessively large deflections were omitted by Carter et al. (2000). Carter et al. (2000) propose that the measured data should be shifted by -5 to -10 mm because a correction was presumably not done for lateral translation, hence the reading is exactly zero at the base. With this in mind, simulation B15 provides the best fit to the data, with deflections of about -25 mm, -32 mm, and -10 mm at the top, middle (i.e. depth = 14 m), and bottom of the diaphragm wall, respectively.



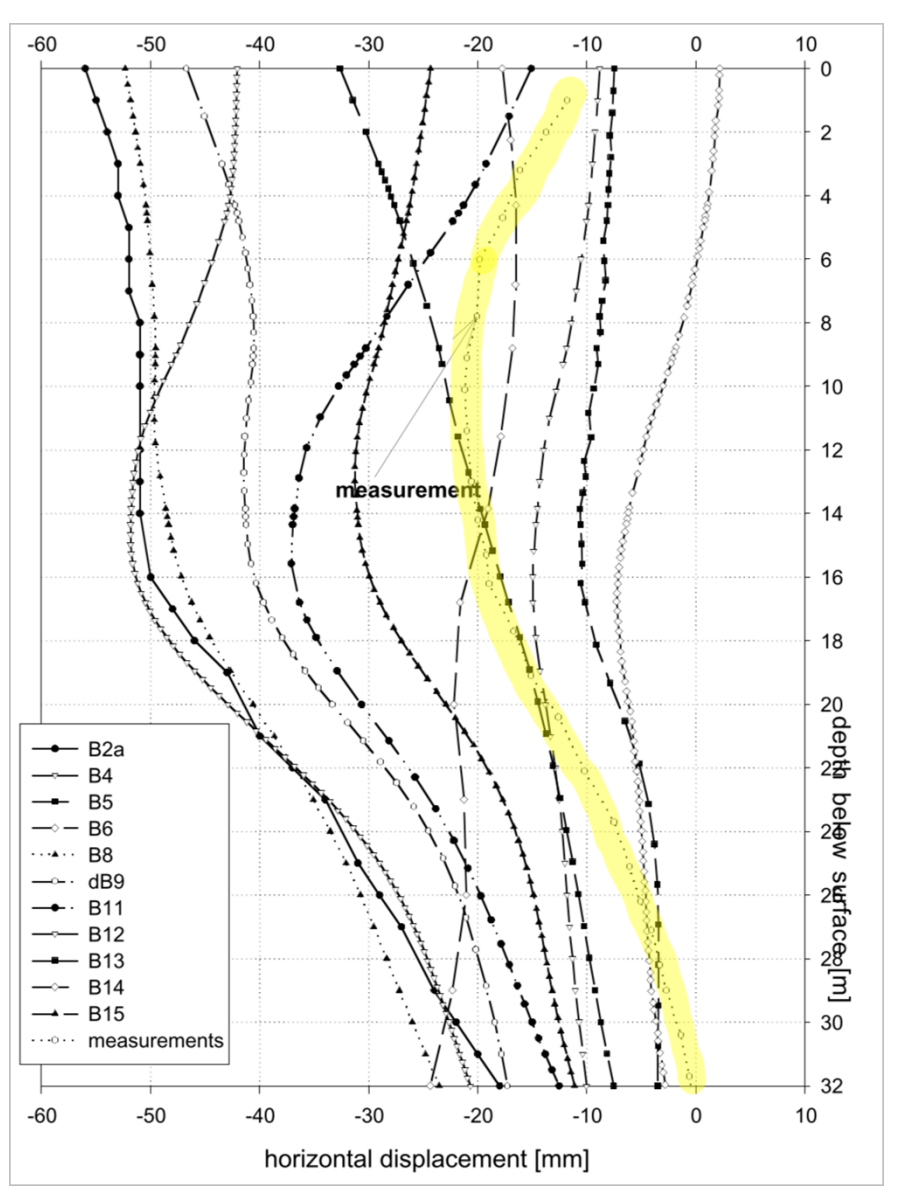


Figure 7. A subset of simulations by consultants and academics compared to the measured wall deflection.

Many of the simulations shown in Figure 7 were completed using the same commercially available computer code and/or constitutive soil model. Carter et al. (2000) note that the scatter can be primarily attributed to 1) assumptions about the spatial variability in stiffness; 2) treatment of the soil at the soil-wall-interface; and 3) the one-step simulation of dewatering. Carter et al. (2000) suggest that (3) contributed to a general over-estimation of the maximum wall deflections but that (1) resulted in the greatest source of error. More specifically, Carter et al. (2000) noted that stiffness values based solely on oedometer measurements were grossly under-estimated, resulting in excessively large simulated deflections. The most realistic simulations used stiffness values that were commensurate with literature-based values.

Excavation analyses involve a predominance of lateral stress relief. As such, the initial horizontal stresses are particularly important. Recall that the initial stresses were established by means of the K0 procedure. The horizontal effective stress are therefore equal to $\sigma'_{xx} = K_0(\sigma'_{yy})$ and that total horizontal stress $\sigma_{xx} = \sigma'_{xx} + u$, where u is the pore-water pressure (refer to the graphs in the associated project file). Larger initial horizontal stresses can intensify the stress



relief caused by excavation; however, they can also result in smaller initial deviatoric (i.e. shear) stresses. The later may increase the soils ability to resist shear, thereby limiting the load transfer onto the wall during excavation. As such, careful attention should be paid to the establishment of the initial stresses. A sensitivity study could be conducted to determine the role of K_0 on the simulated deformation patterns.

Dewatering of the excavation causes a decrement of water pressure within the area bounded by the diaphragm wall and hydraulic barrier (Figure 8). The pore-water pressure conditions within this area are hydrostatic. The pore-water pressure at the base of the hydraulic barrier (i.e. y-coordinate = 28 m) remains elevated; consequently, the uplift pressure at the end of construction would have to be given careful consideration during the design stage. Contours of total head reveal that flow is occurring under the diaphragm and through the hydraulic barrier, albeit at a minimum rate (refer to the associated project file).

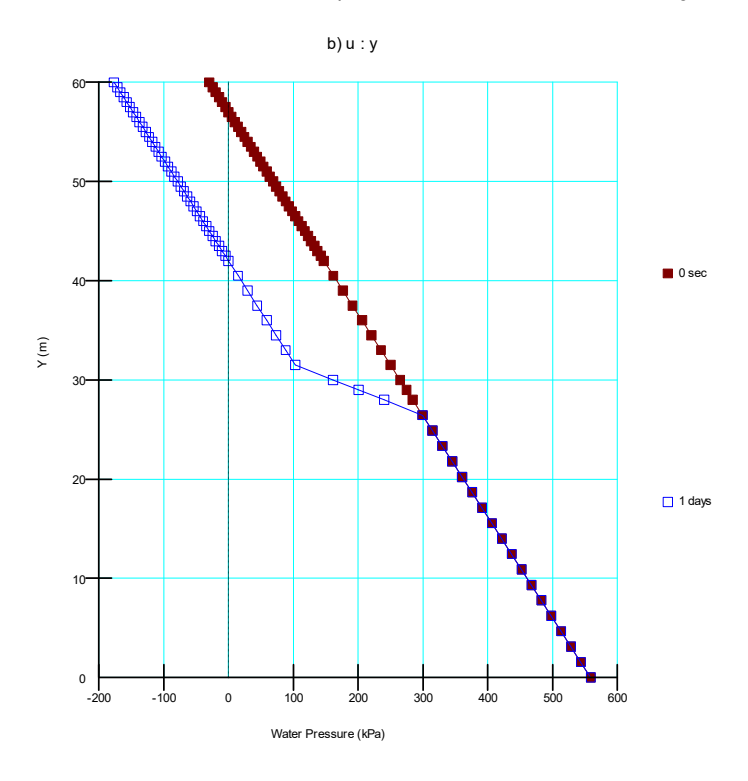


Figure 8. Water pressures before and after the dewatering stage: left boundary.

Figure 9 shows the wall deflections caused by dewatering for the analyses involving the Mohr-Coulomb model. The decrement of water pressure produced by dewatering caused an increment in the effective stresses within the excavation area (Figure 10), which in-turn results in volumetric compression, causing the wall to deflect even before excavation commences. These deflections are only a by-product of the numerical procedure adopted to reduce the porewater pressure within the excavation and as a result to do reflect the response of the physical system. The accumulated displacements and strains were therefore reset in the subsequent load-deformation analysis (refer to the associated project file).



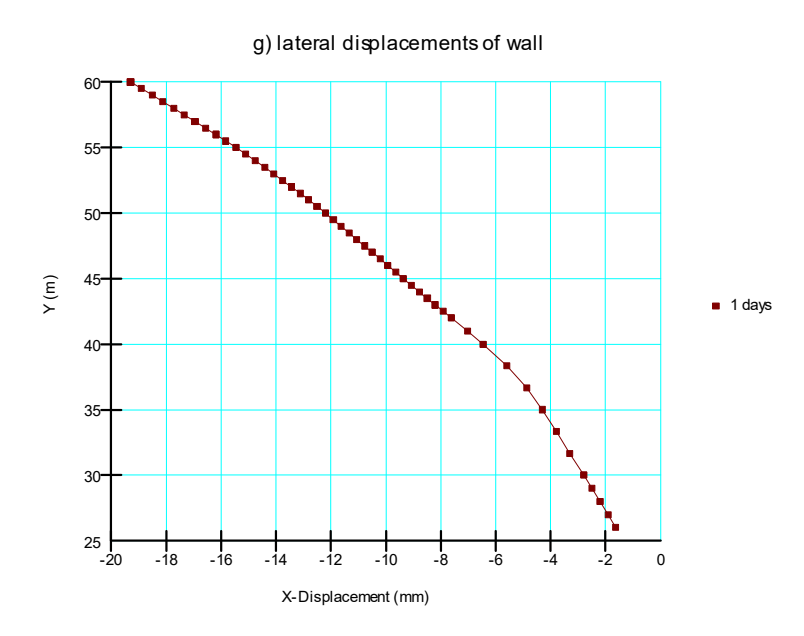


Figure 9. Wall deflections caused by dewatering

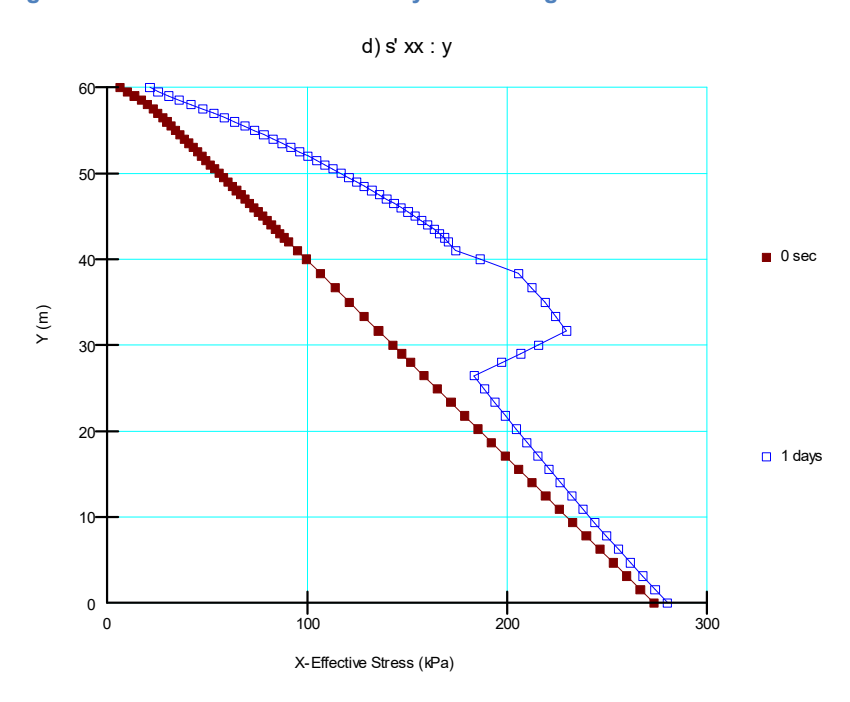


Figure 10. Horizontal effective stress before and after dewatering: left boundary: Mohr-Coulomb model.

Figure 11 shows the wall deflections caused the first two stages of excavation and the installation of the upper row of anchors. The wall deflects to the left during excavation and then pre-stressing of the anchor causes the wall to bend back to the right (Day 4; Figure 11). Figure 12 shows the wall deflections from Day 4 (i.e. installation of the upper row of anchors) through to the installation of the middle row of anchors (Day 7). Figure 13 shows the wall deflections from Day 7 (i.e. installation of the middle row of anchors) through to the installation of the lower row of anchors (Day 10) and to the final stage of excavation (Day 11). The pronounced effect of pre-stressing of the middle (Day 7) and lower (Day 10) rows of anchors is readily apparent. Note



also that the most pronounced increment in wall deflections occurs during the last stage of excavation (Day 10 to Day 11), regardless of the material model used in the simulation.

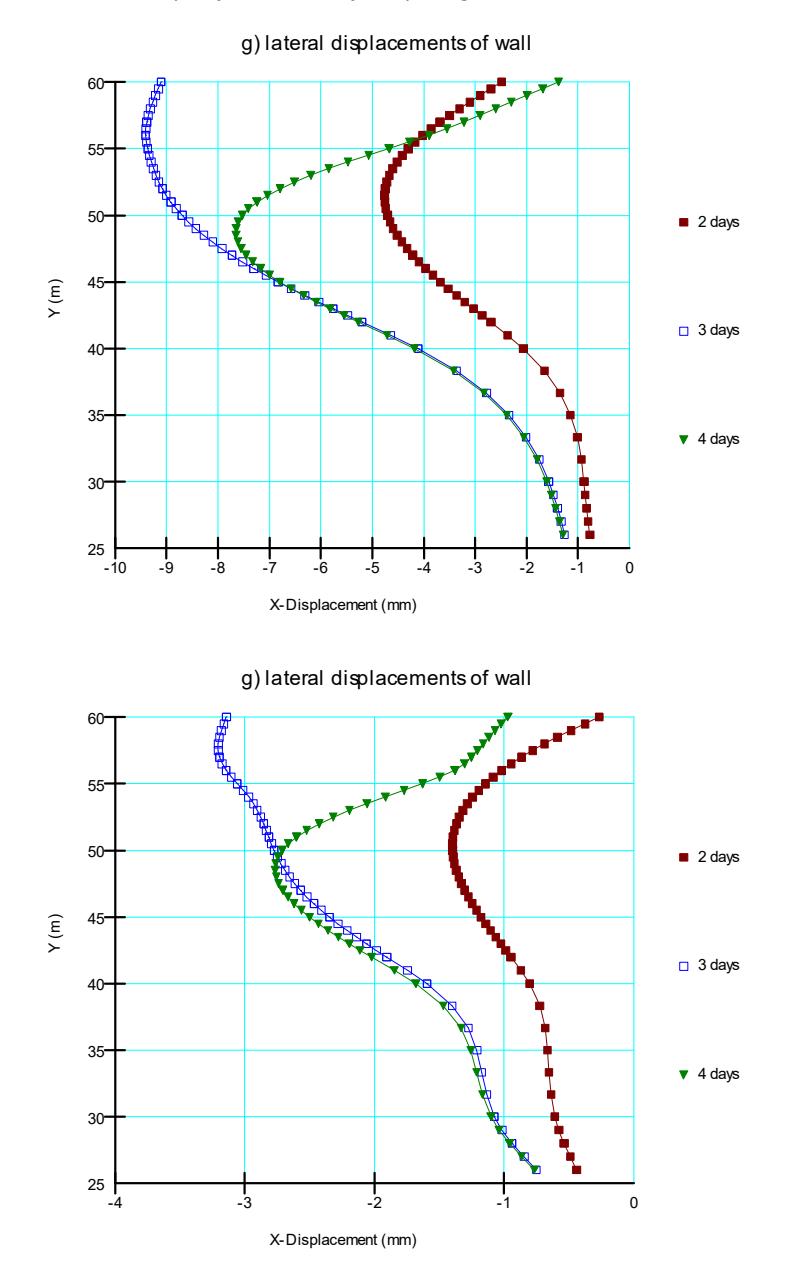


Figure 11. Wall deflections from the stage 1 and 2 of excavation and pre-stressing of the upper row of anchors: Mohr-Coulomb (top) and Hardening Soil (bottom).



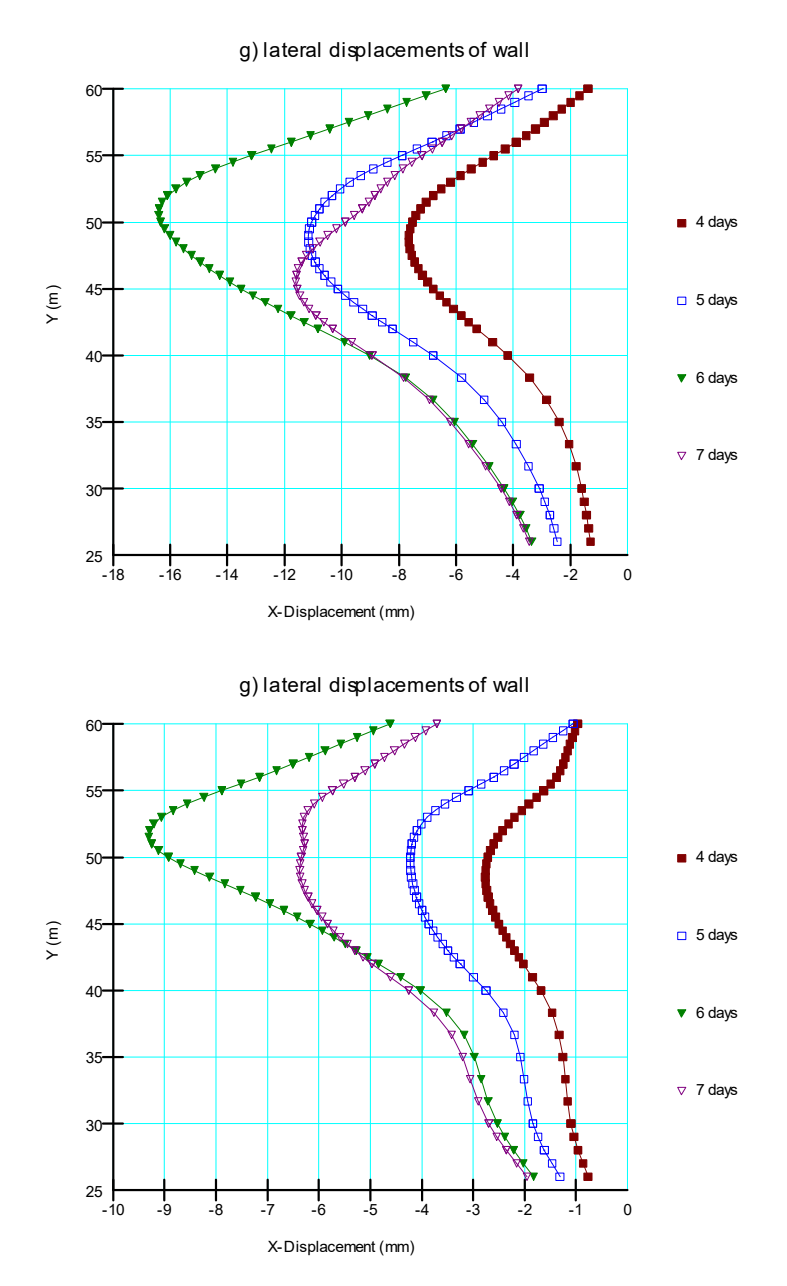


Figure 12. Wall deflections from the Day 4 to the pre-stressing of the middle row of anchors at Day 7: Mohr-Coulomb (top) and Hardening Soil (bottom).



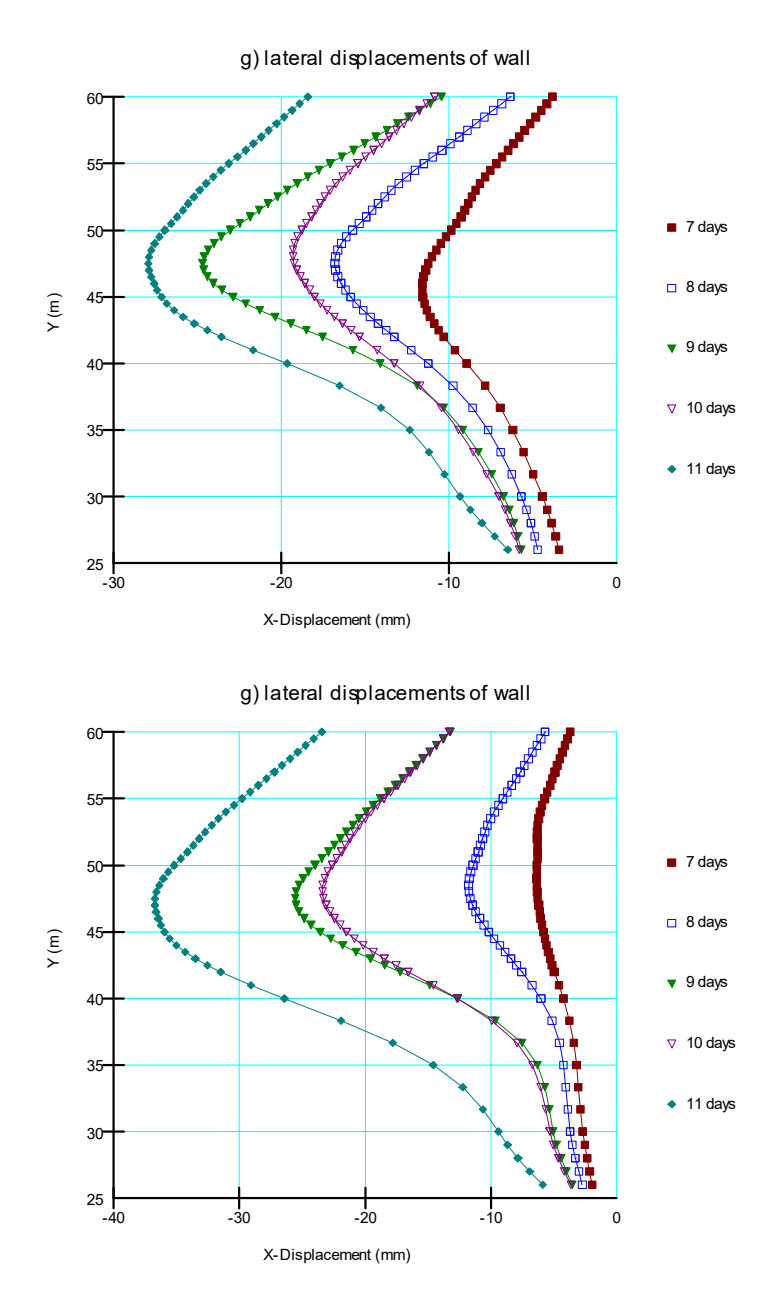


Figure 13. Wall deflections from the Day 7 to pre-stressing of the lower row of anchors (Day 10) and the final stage of excavation (Day 11): Mohr-Coulomb (top) and Hardening Soil (bottom).

Figure 14 compares measured deflections with the simulated values at the end of construction. Recall that the simulated values do not include the deflections caused by dewatering (Define – Project – Analysis: 2 – excavate to 57 – Reset displacements and strains). The simulated maximum deflection and pattern of deflections by both models reasonably map the measured values, which is rather remarkable given that the wall only displaced by about -32 mm – that is, 3.2 cm or 0.032 m – over an excavation depth of nearly 17 m. Similar patterns of simulated behaviour can be seen Figure 7.



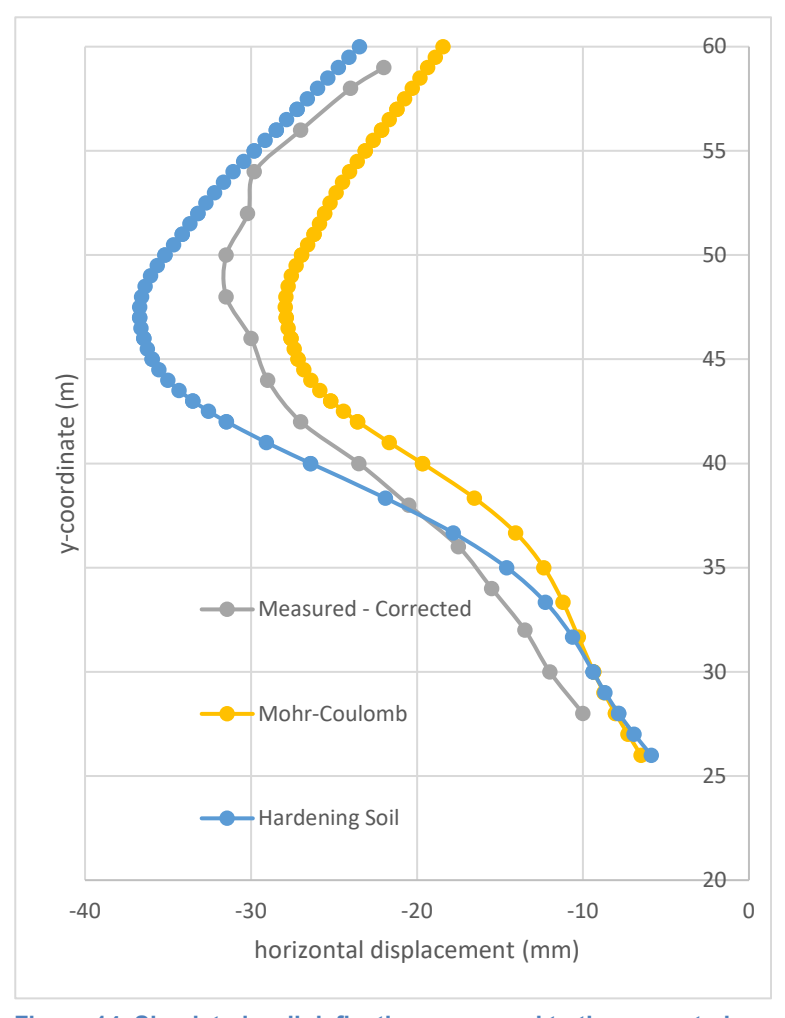


Figure 14. Simulated wall deflection compared to the corrected measured wall deflection.

An important consideration in the design tie-back wall is the maximum bending moments. Figure 15 shows the bending moments at all stages of the simulation. The maximum bending moments are generated after excavating to 45 m (Day 9). The subsequent installation of the lowest row of anchors reduces the bending moments, which then increase marginally after the final stage of excavation. The key realization from these results is that the maximum bending moments may not occur at the end of the excavation.



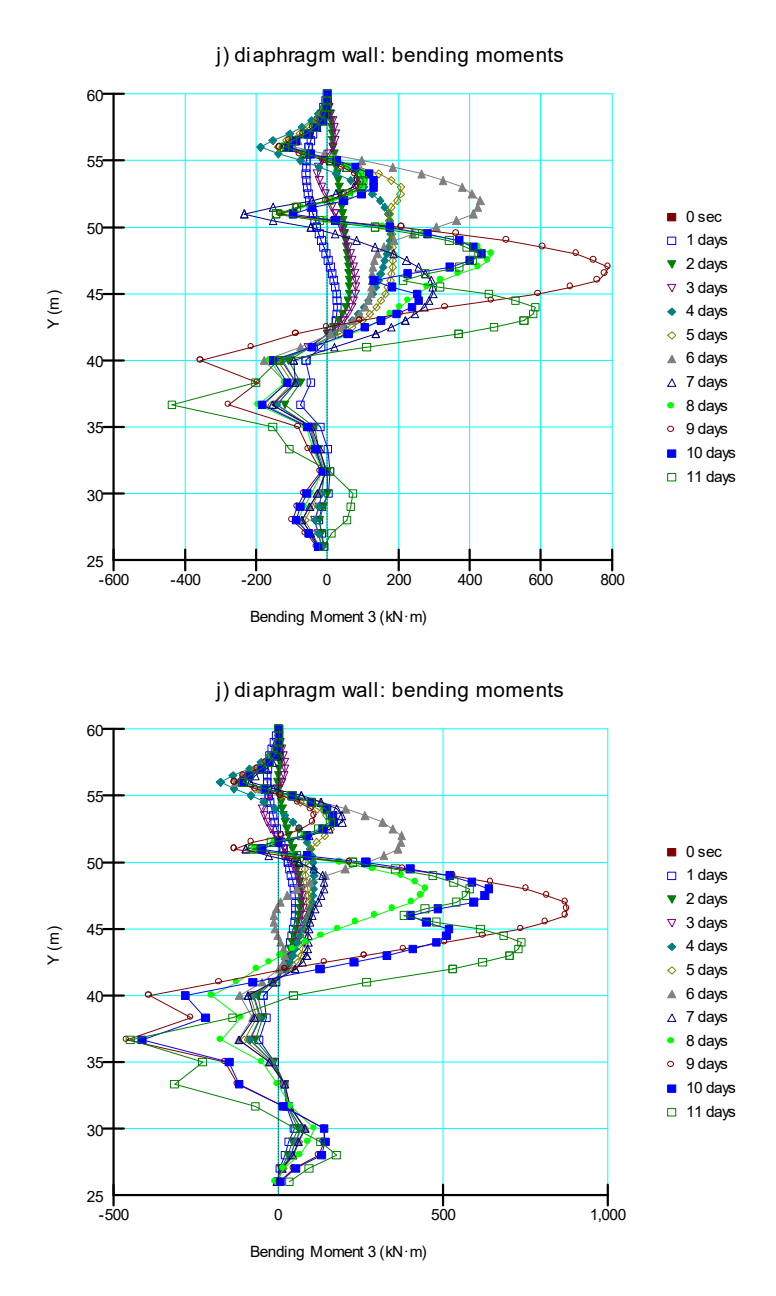


Figure 15. Wall bending moments: Mohr-Coulomb model (top) and Hardening Soil model (bottom).

Figure 16 shows the simulated forces in the free length of the upper anchor. Figure 17 shows a number of selected solution presented by Carter et al. (2000). The initial force of -334 kN corresponds to the tensile pre-stress. The force in the bar has a repeating pattern: the tension increases (i.e. decreases in magnitude) during excavation but decreases (i.e. increases in magnitude) when a lower level of anchors are pre-stressed. The changes in magnitude during excavation are, however, negligible in the upper row of anchors. The effect is more pronounced in the middle row (refer to the project files). As with bending moments, the maximum tensile force may not occur at the end of the excavation.



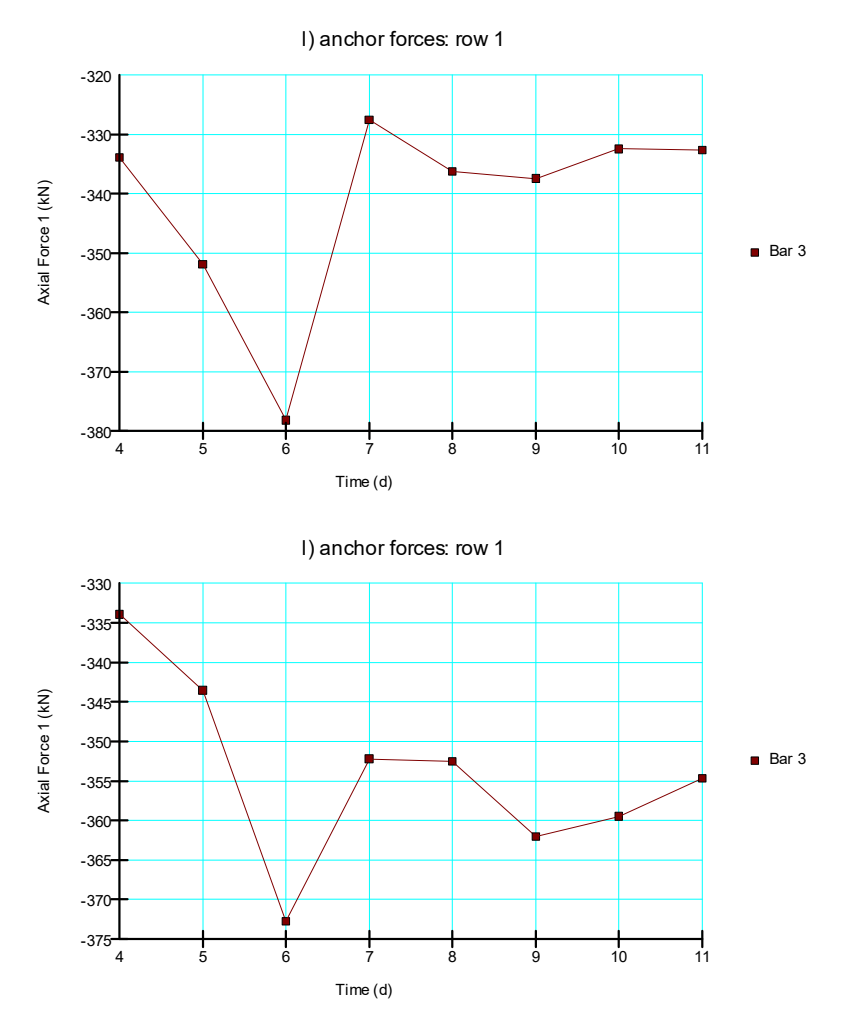


Figure 16. Simulated axial force in the upper anchor: Mohr-Coulomb model (top) and Hardening Soil model (bottom).



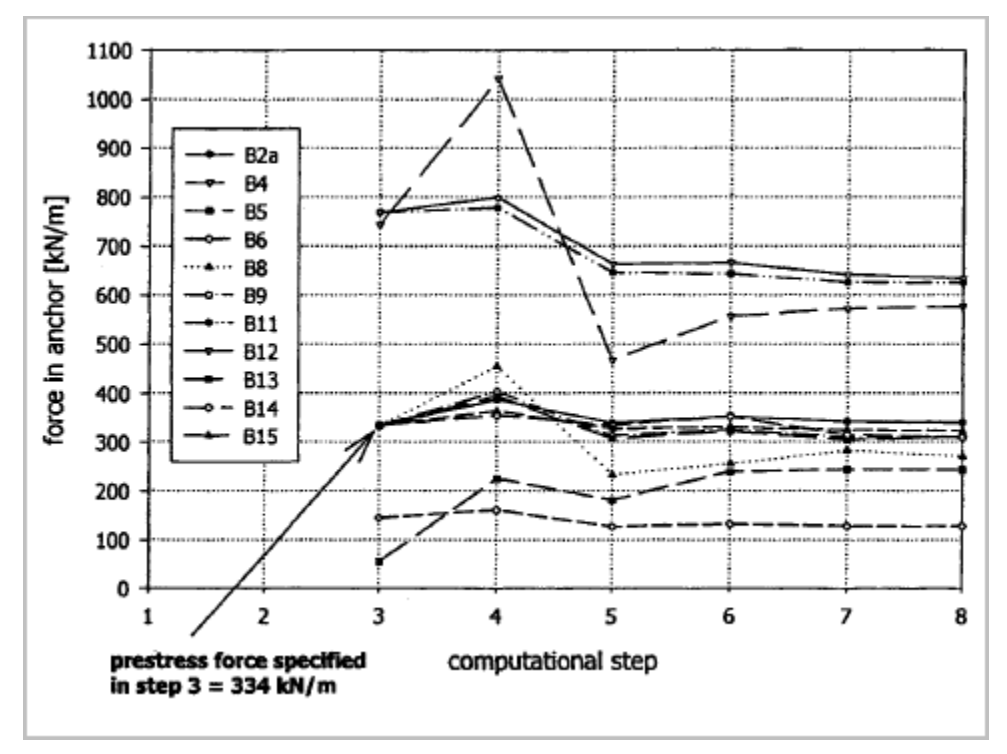


Figure 17. Forces in the first row of anchors for selected solutions presented by Carter et al. (2000)

Figure 18 shows the ground surface displacements outside the excavation. Carter et al. (2000) indicated that simulated displacements corresponding to the results in Figure 7 varied between settlements of 50 mm to surface heaves of about 15 mm. Carter et al. (2000) described the discrepancy as disappointing because, in the author's opinion, one of the main goals of such an analysis is the prediction of settlement. The discrepancies were attributed to modelling assumptions; however, numerical errors may have also played a role in some cases.



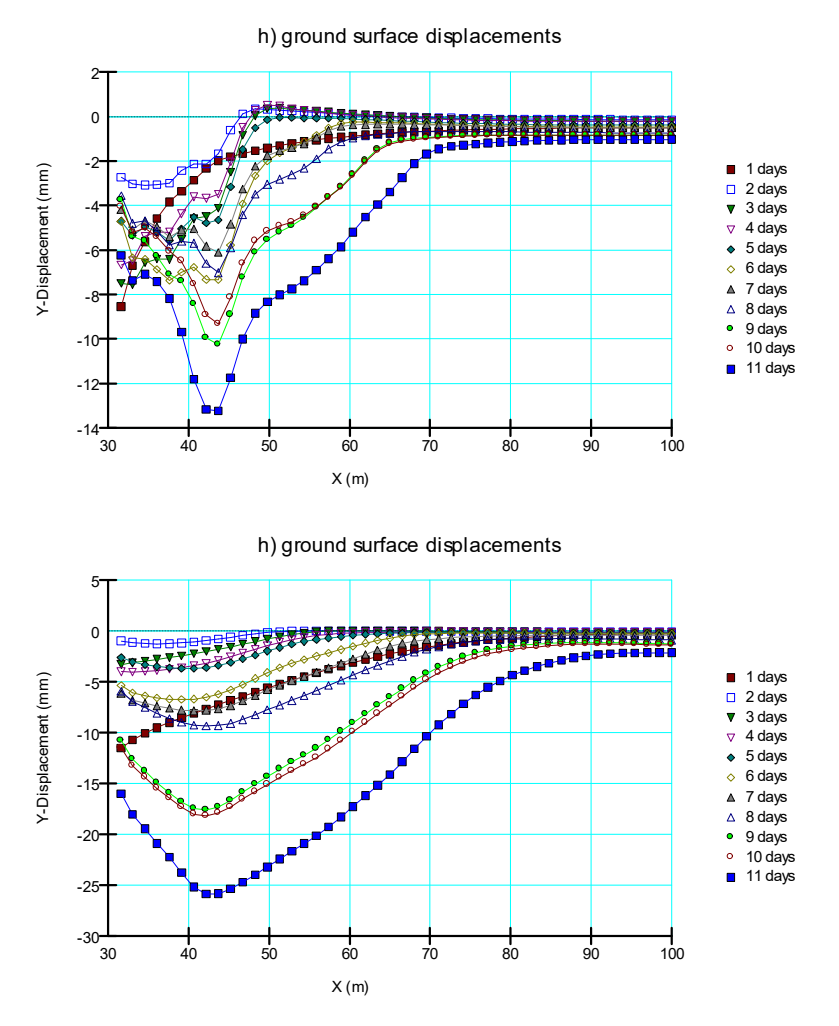


Figure 18. Ground surface displacements: Mohr-Coulomb model (top) and Hardening Soil model (bottom).

One aspect of shoring wall construction that the modeling does not capture is the loss of ground behind the wall. This can be particularly problematic in a pile-lagging system, where portions of the excavation face are exposed for a period of time before the lagging is installed. Furthermore, there may be some settlement before the lagging picks up the load; that is, slack in the system. In the case of a carefully constructed diaphragm wall, there is likely little or no loss of ground behind the wall. As a very broad principle, more expensive shoring systems like diaphragm walls are used in cases where settlement outside the wall is a major concern. Less expensive systems like piles with lagging are used when settlement is less of a concern. The point is that the potential for settlement is related to the shoring system behavior and the installation procedures. The modeling, unfortunately, cannot capture all physical behaviours manifest during the construction of a shoring wall, particularly in relation to ground loss or softening. The results of the simulation, however, still hold value, particularly in regards to global stability, structural integrity, and reasonable deformation patterns.

Summary and Conclusions

Carter et al. (2000) note that a lot of experience is required in order to make sensible assumptions for material and model parameters, which are not explicitly known beforehand, in order to arrive at a reasonable model of the real situation in the field. The SIGMA simulations lend creditability to this statement given the accuracy of the predictions, which resulted from



proper parameterization. It is worth noting; however, that there are other aspects to the use of numerically modelling besides prediction; specifically, that it facilitates the study of physical systems. In fact, it could be argued that the ability to study physical systems is more insightful and valuable to practicing engineers (Krahn and Barbour, 2006). Consider, for example, that the simulation could have been used to gain a better understanding of the most important soil/structural parameters and the effects of dewatering on wall deflection prior to excavation. The simulation results could in-turn inform laboratory and/or in situ testing and the dewatering design. The numerical model could also have been refined to gain an even better understanding of the physical system.

References

Carter, J.P., Desai, C.S., Potts, D.M., Schweiger, H.F. and Sloan, S.W. 2001. Computing and computer modelling in geotechnical engineering (Invited paper). Proceedings of the International Conference on Geotechnical and Geological Engineering (GEOENG 2000), Melbourne, volume 1, p. 1157-1252.

GEOSLOPE International Ltd. 2020a. Stress-strain modeling with GeoStudio 2021. Calgary, Alberta, Canada.

GEOSLOPE International Ltd. 2020b. Heat and mass transfer modeling with GeoStudio 2021. Calgary, Alberta, Canada.

Krahn, J.K. and Barbour, S. L. 2006. The Purpose of Numerical Modelling. Geo-Strata. July/August Issue.

